J. Agromet Indonesia 21(2) : 12-26

ANTHROPOGENIC CHANGES ON LAND COVER AND ITS IMPACT ON ACTUAL EVAPOTRANSPIRATION

(Perubahan Antropogenik Penutupan Lahan dan Dampaknya Terhadap Evapotranspirasi Aktual)

E. Runtunuwu

Indonesian Agroclimate and Hydrology Research Institute

ABSTRAK

Tulisan ini memaparkan perubahan distribusi vegetasi akibat kegiatan manusia serta dampaknya terhadap perubahan evapotranspirasi aktual di Monsoon Asia. Perbandingan antara vegetasi aktual dan potensial menjadi indikator dari dampak perubahan akibat kegiatan manusia. Kondisi vegetasi akual diidentifikasi dengan menggunakan citra satelit, sedangkan vegetasi potensial diekstrak dengan menggunakan data iklim. Dengan membandingkan distribusi vegetasi antara potensial dan aktual, ternyata bahwa perubahan banyak terjadi di India, China, Indonesia dan Malaysia. Selanjutnya, dengan menggunakan analisis neraca air dilakukan perhitungan evapotransipirasi aktual untuk kedua kondisi tersebut dengan menggunakan data iklim yang sama, tetapi dengan nilai albedo yang berbeda sebagai penciri perbedaan antara kondisi vegetasi potensial dan actual. Perubahan E_a berkisar antara 0-12% per tahun. Nilai 0 untuk mencirikan daerah yang tidak mengalami perubahan akibat kegiatan manusia. Penurunan E_a sebesar kurang dari 5% teridentifikasi di daerah yang mengalami perubahan dari *evergreen broadleaf forest (seasonal)* ke padi sawahataupun dari hutan subtropikal menjadi lahan pertanian, seperti yang terjadi di Shandong (China), Uttar Pradesh (India). Penurunan E_a mencapai 9% teridentifikasi pada saat hutan sub tropis berubah menjadi padi sawah, seperti yang terjadi di Assam (India), serta Guangdong dan Guangxi (China). Penurunan sebesar 12% terjadi pada saat hutan tropis berubah menajdi lahan pertanian seperti yang terjadi di Kalimantan Selatan (Indonesia) and Pahang (Malaysia).

Kata kunci: Vegetasi potensial, vegetasi aktual, evapotranspirasi aktual, dataset global dan Monsoon Asia.

ABSTRACT

The study described the land cover/vegetation changes that have occurred due to human activities and its impact on actual evapotranspiration in Monsoon Asia. Comparison between current and potential vegetation that indicates impact of human activities indice. Current vegetation was identified using satellite data, and potential vegetation is extracted using climate data. By comparing current and potential vegetation, showed that a lot changes have been happened in India, China, Indonesia and Malaysia. Then, by using water balance analisys is calculated actual evapotranspiration for both condition by using similar climate data, but different albedo value as the determination og the difference between current and potential vegetation. Change of E_a ranged between 0-12% per year. Value 0 is indicated area that did not get change due to human activities. Decrease of E_a less thab 5% is identified in area that have changed from *evergreen broadleaf forest (seasonal)* to ricefiled or from sub tropical forest to agriculture land like in Shandong (China), and Uttar Pradesh (India). Decrease of until 9% is indentified when sub tropical forest is change to

Penyerahan naskah : 8 Juni 2007
Diterima untuk diterbitkan : 9 September 2007

be ricefiled like in Assam (India), Guangdong dan Guangxi (China). Decrease until 12% is happened when tropical forest changed to be agriculture land like in South Kalimantan (Indonesia) and Pahang (Malaysia).

Keyword : Potential vegetation, current vegetation, actual evapotranspiration, global dataset, and Asian Monsoon .

INTRODUCTION

Knowledge of the evapotranspiration is important in global change research since this parameter is essential to the hydrological and climatic processes between the earth and atmosphere, which are performed by heat and water balance equations. Therefore, many researches have been focused not only on the microclimate aspects, but also in the regional, continental, and global level.

Relating to study of the land cover change and its impact on hydrologic changes especially for evapotranspiration parameter recently has been seriously observed, as reported by Running *et al*. (1996): Dickinson and Henderson-Sellers in 1988 simulated the Amazon basin with full forest cover, and then replaced with grasslands. The degraded grasslands reduced evapotranspiration so much that surface temperatures were predicted to increase by 3-5°C; Walker *et al*. in 1995 found that precipitation had been reduced by 1.2 mm/day due to reductions in evapotranspiration of 18% by land cover changes. Running *et al*. (1996) also pointed out that the global hydrologic changes resulting from land cover changes are predominantly of two kinds. The evapotranspiration was decreased when forested areas were changed to cropland and it was increased when the deserts were modified to irrigation land. Kondoh (1995) pointed out that over Monsoon Asia the potential evapotranspiration was changed around 0-200 mm/year because of land cover changes by human activities.

Following those research evidences, the purpose of this study is to investigate the land cover/vegetation changes that have occurred due to human activities and its impact on actual evapotranspiration in Monsoon Asia (-20°S -60°N, 60°E-160°E).

METHODS

To allow for land cover and E_a comparisons, the method was defined in two ways (Figure 1). The first is the current vegetation procedure that indicates the current vegetated surfaced determined with satellite data. The second way is potential vegetation that exists the vegetation distribution without human disturbance determined with climatic data. The difference between the two results of vegetation distributions and E_a calculations are then mapped for comparisons.

Current vegetation classification

An alternative way to obtain the current vegetation distributions is by means of satellite data. Solar radiation in the visible and near-infra red wave bands reflected by the Earth's surface and collected by remote sensing, can be combined into a spectral vegetation index such as the Normalized Difference Vegetation Index (NDVI) and related to the physical properties of the vegetation. The NDVI is generated from red and near-infrared (NIR) reflectance of satellite sensor by the following equation: (NIR-red)/(NIR+red). High values of this index are obtained for areas covered by green vegetation and low values for unvegetated areas and cloud covered.

There were some attempts to use the NDVI value for deriving land cover grouping at a continental or global scale. Some researcher applied the single or multi temporal datasets of the NDVI to land cover classification for Africa (Tucker, *et al*., 1985), Asia (Malingreau, 1986; Tateishi, 1997), Southeast Asia (Achard and Estrequil, 1995), Africa (Townshend and Justice, 1986), and global (DeFries and Townshend, 1994).

However, in this study, we combine the NDVI and the climatic data, since we consider the differences in climatic condition are able to show either the latitudinal or longitudinal variations associated with the distribution of vegetation. Therefore, the twelve monthly of each NDVI, temperature and precipitation data were applied together using unsupervised and maximum likelihood algorithm in order to obtain the homogeneous phenology classes for current land cover classification.

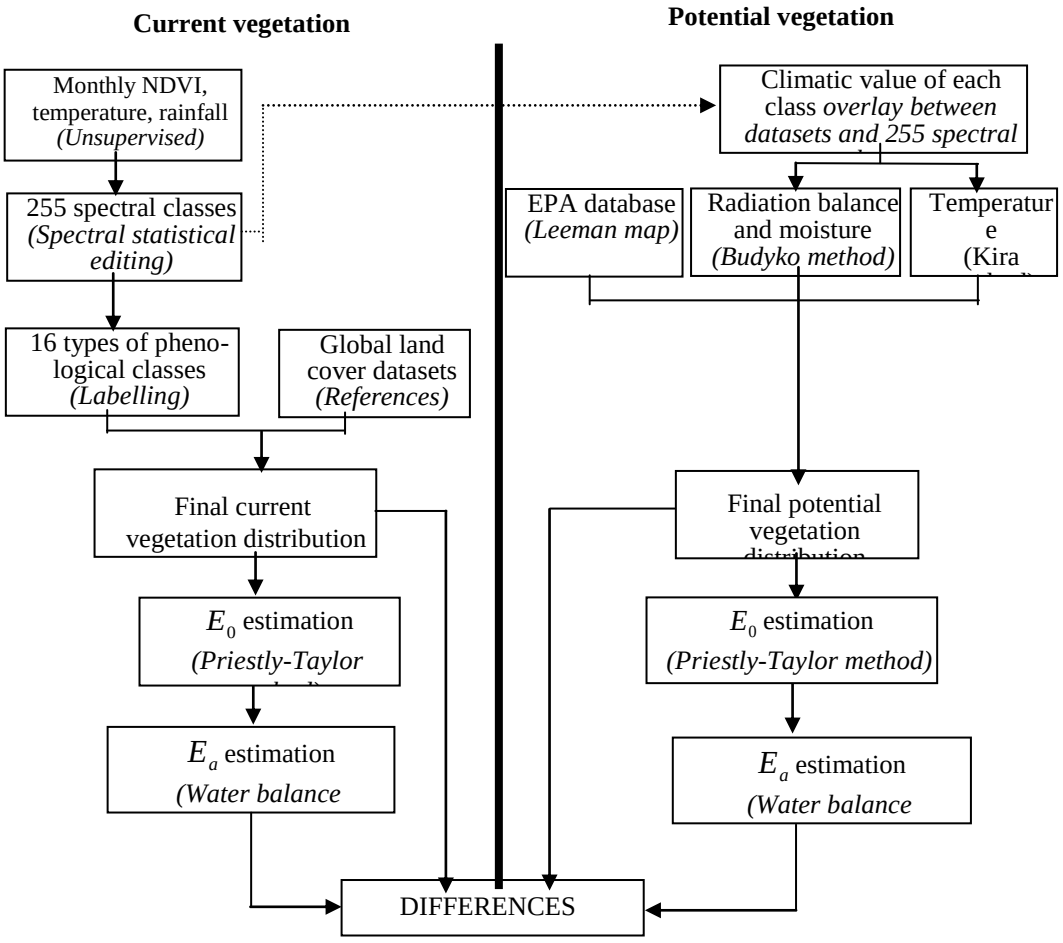

Figure 1. Schematic procedures used on this study.

Potential vegetation classification

The next procedure after determination of the current vegetation distribution is to analyze the potential vegetation for the same vegetation class. By assuming the same phenology class resulted from previous step will have the same hydrological function, the temperature, cloudiness, precipitation, radiation, humidity index, as well as elevation of each class have been extracted from available ground-based global datasets. These extracted climatic data were applied to determine the distribution of potential vegetation by using Kira (1948) and Budyko (1974) methods. The two maps resulted were then compared with Leemans (1990) map to conclude the potential vegetation of each class.

Kira (1945) introduced the Warmth Index (WI) concept to divide the Monsoon Asia region into seven main regions. Kira`s WI was defined as: WI =∑(Ti-5), where, i=1 to 12, $T_i > 5$, and T_i is the monthly temperature (°C). The WI value of each class was then associated with the following criteria to determine the type of its own forest. Thus, less than 0 is generally associated with the polar frost zone; between 0 and 18 with polar (tundra zone); between 18 and 45 with sub polar; between 45 and 85 with cool temperate; between 85 and 180 with warm temperate; between 180 and 240 with sub tropical, and more than 240 with tropical zones.

Budyko (1974) used both the radiation balance and moisture condition in geographic zonality. A moisture condition in similarity with humidity index was calculated by dividing the evaporation and precipitation. Thornthwaite's (1948) method was applied to calculate the evaporation, which uses air temperature as minimum input requirement. Budyko's method divided a zone in to 8 main groups or 22 sub regions. Detailed procedure of the classification method could be referred to Budyko (1974).

Leemans (1990) created the Global Holdridge Life Zone Classification using bio-temperature, mean annual precipitation, and E_0, resulted in 38 different kinds of vegetation forms for whole the world. These image data could be extracted from NOAA/NGDC and EPA Disc A (1992) directly.

E_a estimation

The E_a has been calculated as a residual in water balance equations from estimates of potential evapotranspiration, E_0, using a soil moisture reduction function as shown in Figure 2 that modified from Ahn (1995). There exist many methods for computing E_0, which have been developed from different kind of climatic input data (Kondoh, 1994, Jensen *et al*, 1990).

Because of the limited of available spatial image datasets, the E_0 in this study was calculated by using Priestly-Taylor method (1972). One assumption of this method is in the absence of advection condition, E_0 (mm), can be estimated from:

$$E_0 = \alpha \cdot Er \cdot \Delta/(\Delta + \gamma) = \alpha \cdot (R_n - G) \cdot \Delta/(\Delta + \gamma) = \alpha \cdot ET_{eq}$$

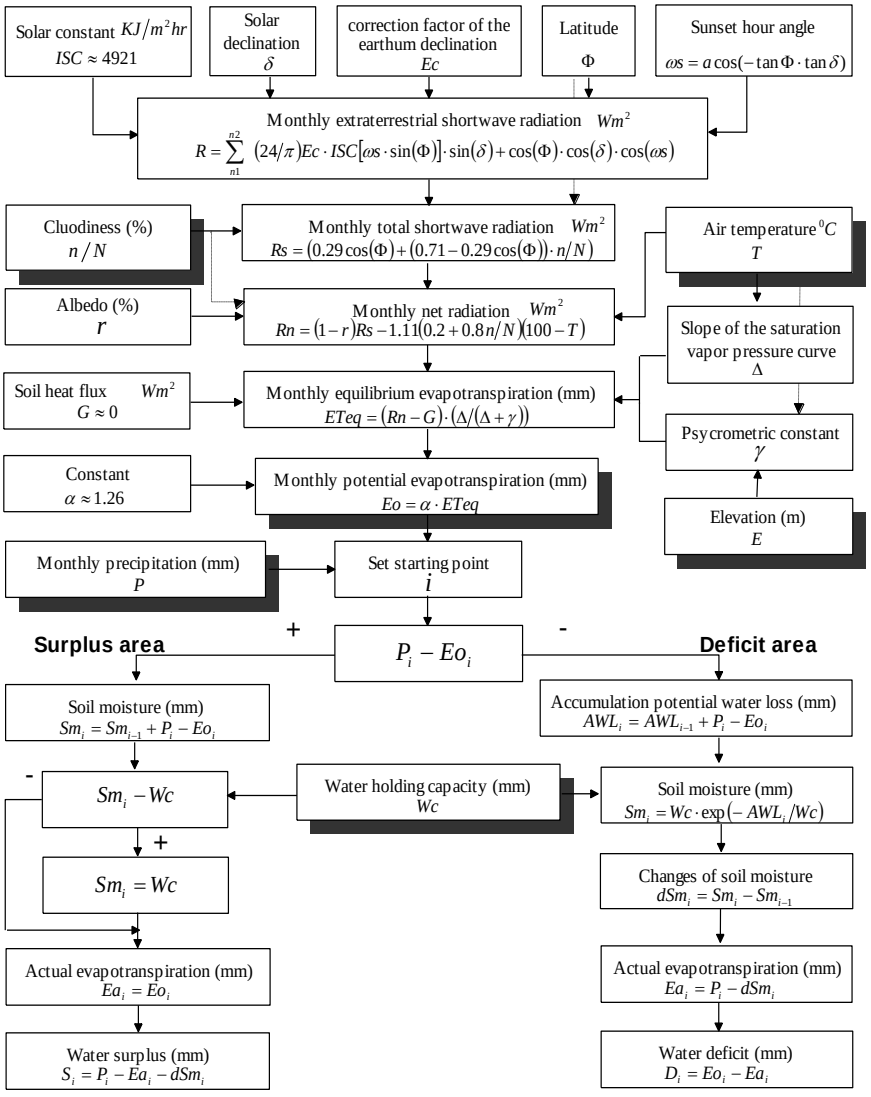

$$Ec = 1.00011 + 0.03422\cos(\Gamma) + 0.00128(\Gamma) + 0.000719\cos(2\Gamma) + 0.000077\sin(2\Gamma)$$

$$\Gamma = 2\pi(dn - 1)/365$$

$dn =$ day number of the year (1-365)

$n1, n2 =$ day numbers at the beginning and end of the month

$$\Delta = \frac{4098.0258 \cdot 6.11 \cdot \exp((7.5T)/237.3 + T)}{(237.3 + T)^2}$$

$$\gamma = \frac{[1005(1013.25 - 0.11986E + 0.000005356E^2)]}{[622(2501 - 2.37T)]}$$

Figure 2. A flow chart for monthly E_a computation by water balance approach.

Where R_n and G are net radiation and heat flux density (W/m^2), respectively; E_r is rate of net radiation (W/m^2), α is constant (1.26); Δ is the gradient of the saturated vapor pressure at a certain air temperature; γ is the psychometric constant; The weighting factor $\Delta/(\Delta+\gamma)$ is unit less; ET_{eq} as the equilibrium evapotranspiration (mm) is defined as follows:

As shown in equation (1) and (2), net radiation, R_n, is a major variable of Priestly and Taylor method. Therefore, the reliability of the E_0 estimation is depended on accuracy of this variable.

$$ET_{eq} = \Delta \cdot (R_n - G)/(\Delta + \gamma)$$

Ahn and Tateishi (1994) used the Linacre method to calculate R_n:

$$R_n = (1-r)R_s - 1.11(0.2 + 0.8\,n/N)(100 - T)$$

where R_s is total (direct and diffuse) short wave solar radiation (W/m2), n/N is the ratio of actual and maximum possible sunshine hours (%). T is temperature (oC) and r is albedo (%). The result of monthly E_0 analysis has been used together with monthly precipitation and soil water holding capacity (W_c) on the next step to calculate E_a, as shown in Figure 2.

Firstly, when the monthly E_0 is reduced with precipitation in mm/month (P), it is possible to obtain a clearer understanding of the times (as staring point i) of moisture deficiency and access, and the relative moistness or aridity of the climate. In those stations where precipitation in every month is greater than the potential evapotranspiration, the soil always remains full of water and a water surplus occurs. At other stations where precipitation is always less than potential evapotranspiration, there is not enough water for the vegetation to use and a moisture deficit occurs.

Secondly, the soil moisture status of each month, i, in mm/month, was calculated with accumulated potential water loss (AWL) and water holding capacity (W_c), as follow:

if $P_i - E_{0_i} = negatif$

$$AWL_i = AWL_{i-1} + P_i - E_{0_i}$$

$$S_{m_i} = W_c \ \exp(-AWL_i / W_c)$$

else

$$S_{m_i} = S_{m_{i-1}} + (P_i - E_{0_i})$$

(4)

W_c is obtained from the available global dataset.

Thirdly, the E_a can be derived from the rates of P, E_0, and S_m in following way:

if $P_i - E_0 = negatif$

$$E_{a_i} = P_i - (S_{m_i} - S_{m_{i-1}})$$

else

$$E_{a_i} = E_{0_i}$$

Detail procedure of the E_a estimation used in this study could be referred to Thornthwaite and Mather (1957) and Ahn (1995).

DATASETS

To achieve the goal of this study, the data used in this study as following:

a. NDVI data: It was compiled from the Time Series of 0.144º Global Monthly Vegetation Cover from NOAA/AVHRR CD-ROM Ver. 1.0 (http://perigee.ncdc. noaa.gov).

b. Climatic data of temperature, cloud cover, radiation, and precipitation: The Climatic Research Unit, University of East Anglia has supplied CRU05 0.5 Degree 1901-1990 Mean Monthly Climatology and CRU05 0.5 Degree Monthly Climate Time-Series (1901-1995), Ver.1. April 1999 (http://ipcc-ddc.cru.uea.ac.uk).

c. Albedo: The data was compiled from a one degree seasonal Mathew Albedo supplied by Global Ecosystem Database, NOAA/NGDC and EPA, Disc A, 1992.

d. Elevation: It was obtained from Global Land One-Kilometer Base Elevation (GLOBE) Digital Elevation Data, NOAA/NGDC, Ver. 1.0 1998 (http://www.ngdc.noaa.gov).

e. Soil water holding capacity was generated by Bouwman Bouwman *et al.* (1993). The data was supplied by UNEP/GRID-Geneva.

To be consistent with the whole datasets, all of the image data were resampled to ten minutes or about sixteen kilometer grid dataset covering Asian region (-20°S -60°N, 60°E-160°E) and were reprojected on a linear latitude longitude grid.

RESULTS

Distribution of current vegetation

Figure 3a shows the distribution of current vegetation. Briefly, the location of some selected classes are described below. The tropical rain forest forms a wide area in Indonesia (Papua, Kalimantan), Malaysia (Sarawak, Sabah), Papua New Guinea (Western, East Sepik), Myanmar/Burma (Shan State, Kachin State), and Philippines (Mindanao). Tropical seasonal forest was distributed in Myanmar (Tenasserim, Karen), India (Uttar Pradesh, Kerala), and Cambodja (Mondol Kiri, Kaoh Kong). Large portions of the other vgtation types are dominated in sub tropical region.

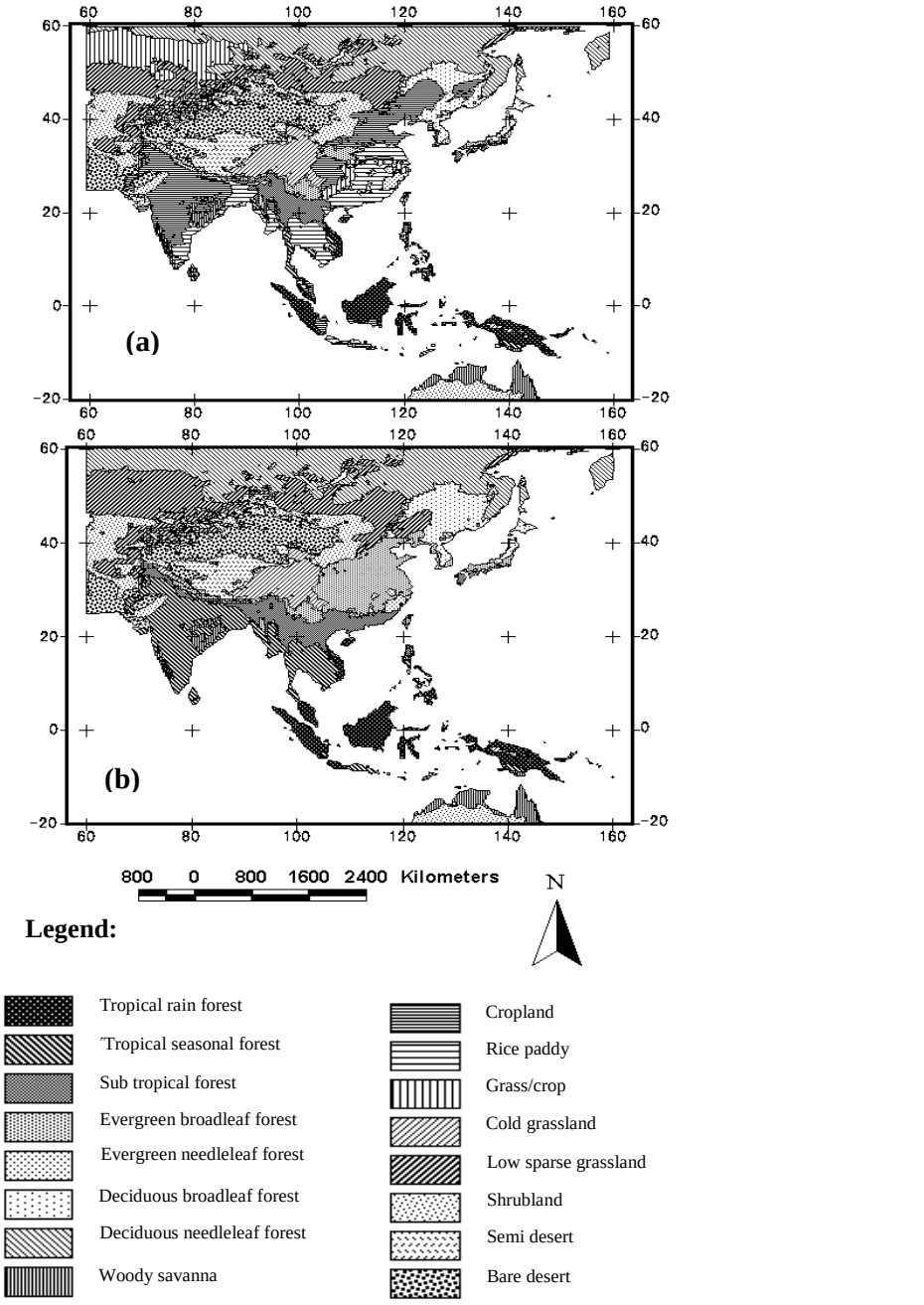

Figure 3. Distributions of (a) current and (b) potential vegetation in Monsoon Asia.

Distribution of potential vegetation

Figure 3b shows the distribution of potential vegetation, which is dominated by forest. The tropical rain forest was distributed in almost whole region of Indonesia, Papua New Guinea, and Brunei. It also appeared in some parts of Philippines, India, and Laos. The tropical seasonal forest was largely distributed in India region and peninsula of Malaya. The largest area of sub tropical forest was distributed in southern China and Myanmar (Sagaing, and Kachin State), and Laos. Evergreen broadleaf forest was mainly distributed in lowland of eastern China, Japan (Chubu, and Kinki), and Myanmar (Chin State and Kachin State). Evergreen needleleaf forest was covered in a small part of Southeastern China (Fujian, Zhejang, Jiangxi, and Jiangxi) beside Kyushu of Japan. The Grassland (low sparse and cold), woody savanna, semi desert shrub, semi desert and bare desert were the same with the current vegetation, since these formation almost no changed.

Estimation of E_a

In order to calculate the amount of E_a change due to the land cover changes by human only or without climatic influences, the E_a of both current and potential vegetations has been calculated with the same climatic input data, except the albedo variable to represent the land cover conditions. Different albedo layer has been utilized here to indicate the differences of both land cover classifications. Hence, the annual albedo of each type of vegetation form was selected and derived from Mathew's Seasonal Albedo (1983) and Katoda`s monthly Albedo (1986).

Figure 4 and Table 1 shows an example of the E_a computation for tropical seasonal forest at Chittagong, Bangladesh. It shows the input data for E_0 estimation based on Priestly and Taylor method, and also the parameter of E_a calculation such as annual value of precipitation (P), water holding capacity (W_c), and soil moisture (S_m). The monthly input data for E_0 estimation, P and W_c were derived from available global datasets, while the S_m, AWL, E_a were estimated by using equations number 4 and 5.

From Table 1, September is determined as initial month or starting point i, since the August was the last month of the period with precipitation more than potential evapotranspiration. Based on Thornthwaite and Mather (1957) because of the sum of all the $P - E_0$ values is positive (221) the value of AWL with which to start accumulating the negative values of $P - E_0$ is 0 (after August). From September to November the precipitation was less than potential evapotranspiration and soil moisture was utilized in evapotranspiration. We expected the runoff did not occur in this period. From December to August, precipitation is greater than potential evapotranspiration. At the time, soil moisture was recharged and runoff begins to occur.

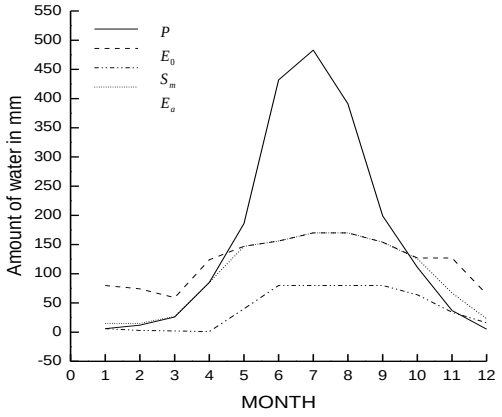

Figure 4. The seasonal fluctuation of precipitation, soil moisture, and evapotranspiration (tropical seasonal forest in Chittagong, Bangladesh)

Table 1. Example of monthly E_a computation for tropical seasonal forest at Chittagong, Bangladesh.

T is air temperature; n/N is cloudiness; E is elevation; r is albedo; P is annual precipitation;

Variable	Jan	Feb	Mar	Apr	May	Jun	Jul	Aug	Sep	Oct	Nov	Dec	Annual
T (^{0}C)	20.5	21.8	26.8	26.8	27.5	27.2	27.4	26.9	27.4	26.8	24.7	20.6	25.4
n/N (%)	36	27	31	32	40	51	59	67	71	66	55	39	47.8
E (m)	104	104	104	104	104	104	104	104	104	104	104	104	
r (%)	11	11	11	11	11	11	11	11	11	11	11	11	11
E_0 (mm)	80	74	59	124	147	156	170	170	147	127	127	65	1445
P (mm)	6	12	26	85	186	432	483	391	199	111	37	5	1975
$P - E_0$ (mm)	-74	-62	-33	-39	40	277	314	221	53	-16	-91	-60	(+) 529
AWL (mm)										-16	-107	-167	
S_m (mm)	6	3	2	1	40	80	80	80	80	64	34	16	487
dS_m (mm)									0	-16	-30	-18	
E_a (mm)	15	15	27	85	147	156	170	170	154	126	67	23	1153

W_c is water holding capacity; AWL is water accumulation potential water loss; S_m is soil moisture; E_0 is potential evapotranspiration, and E_a is actual evapotranspiration.

By applied this approach to 255 classes, the twelve monthly datasets of potential and actual evapotranspiration maps were produced to obtain the annual value for current and potential vegetation conditions. In general, there are some differences between both maps. The latitudinal banding of estimated E_0 results primarily from a large-scale climatic condition. The lowest values are distributed in Russia region (around 200 mm/year), and increased until equator region (more than 1800 mm/year). While based on the E_a map, the value is distributed following the distribution of vegetation type. The lowest values (around 150 mm/year) are distributed in wide desert area of Russia, China, Mongolia, and Kazakhstan. The equatorial zones are bounded tropical regions such as Indonesia, Malaysia, Philippines, Papua New Guinea were associated with the tropical forest with the highest values per year (more than 1600 mm/year). Figure 5 shows also that the E_0 value is higher than E_a. It is ranging from 150 mm/year for tropical rain forest, 386 mm/year for cropland, 273 mm/year for rice paddy, and 800 mm/year for bare desert area.

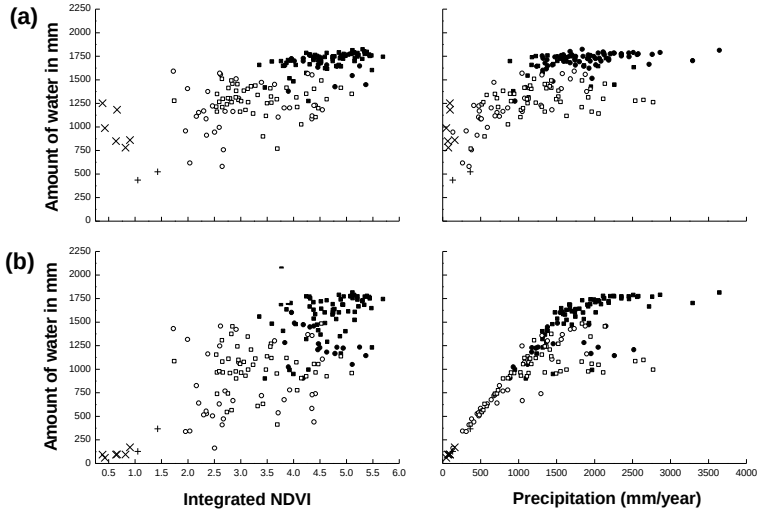

Figure 5. Scatter plots of annual (a) E_0 and (b) E_a versus integrated NDVI and mean annual precipitation of tropical rain forest (■), tropical seasonal forest (•), cropland (O), rice paddy (□), semi desert (+), and bare desert (×).

DISCUSSION

Land cover changed

Areal estimates of current and potential vegetation on the same class have been compared in Figure 9a to indicate which ecosystems have been modified by human activities. The largest focus of the alteration as was expected to be in almost the whole area of India (such as Madya Pradesh, Maharashtra, Andhra Pradesh, Uttar Pradesh, and Rajasthan), Russia (Novosibirsk, Altay, and Omsk), and some parts of China (such as Guangxi, Sichuan, Hunan, Hubei, Nei Mongol, Henan,

Heilongjiang, and Shanxi). This also appeared in Myanmar (Pegu, Irrawaddy, and Magwe), Indonesia (such as Sumatera Selatan, Jawa Timur, Jawa Barat, and Kalimantan Selatan), Kazakhstan (Kustanay, Kokchetav, and Pavlodar), and Pakistan (Punjab and Sind). In other countries such as Papua New Guinea, Philippines, Korea, and Japan, also denoted a little modification.

Considering the type of land cover which has been changed by human activities, we realized that tropical rain forest has been modified to crops was occurred in Indonesia, such as in Kalimantan Selatan and Sumatera Selatan. Some places in Malaysia (Perak), Indonesia (Jawa Barat), and Sri Lanka (Central) show the changes from tropical rain forest to rice paddy area. The tropical seasonal forest that has been changed to crops was occurred in wide area of India (Uttar Pradesh, Madya Pradesh, etc). In Myanmar, I also realized a large area changed from tropical seasonal forest to rice paddy as well in Bangladesh (Khulna), Vietnam (Kien Giang), Cambodia (Preah Vihear), Sri Lanka (Uva, North western), India (Tamil Nadu, Andhra Pradesh). For the sub tropical forest that has been modified to crops was occurred in India (Punjab), while the modified to rice paddy was happened in China (Guangdong, and Guangxi), Bangladesh (Chittagong), and also a little part in Nepal (Bagmati). The evergreen broadleaf forest has been change to crops could be mainly recognized in China (Sichuan, Kiaoning and Guizhou). For other area like Jiangxi, Hunan, and Henan in China, I found that the modification from evergreen broadleaf forest to rice paddy area. I also identified a wide change from deciduous needleleaf forest to grass/crop in Russia (Vovosibirsk). In Kazahkstan such as Kustanay province, the low sparse grassland has been change to grass/crop.

Actual evapotranspiration changed

The amount of E_a changes between potential and current vegetations is 0 to 180 mm/year or 0 to 12% per year, as shown in Figure 6 and Table 2. The 0 value indicates such area where the E_a has no changed, while the positive value indicates the E_a of current condition has been decreased from potential one.

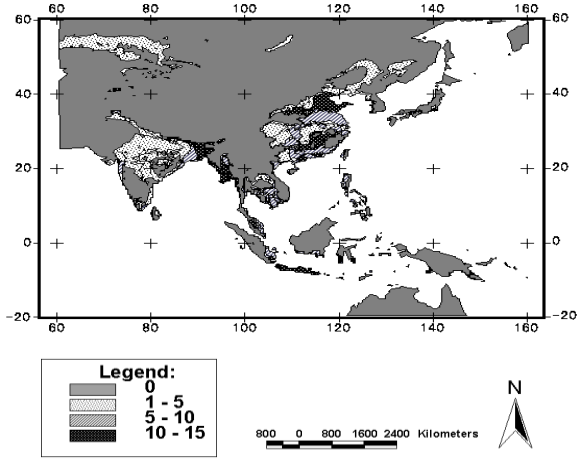

Figure 6. Changes of annual E_a (%) due to land cover changes.

Table 2 presents the recapitulation of mean annual E_a value for some classes of vegetation types, which have been changed by human activities. The highest value (12%) was occurred when the tropical rain forest was changed to rice paddy. The decreased by 9% was happened when the sub tropical rain forest changed to rice paddy. The tropical rain forest which has been changed to cropland caused the E_a decreased by 7% as well as the changed from tropical seasonal forest to rice paddy. The lower value (less than 5%) was happened when evergreen broadleaf forest (seasonal) changed to rice paddy. It also occurred when the subtropical rain forest has been changed to cropland.

Table 2. Mean annual E_a of some vegetation types (a) before and (b) after modified by human activities and its changes.

No	Vegetation types		E_a		
	Potential	Current	a mm/year	b mm/year	Changed (a-b) mm/year (%)
1.	Tropical rain forest	Rice paddy	1527	1346	181 (12)
		Cropland	1506	1394	112 (7)
2.	Tropical seasonal forest	Rice paddy	1136	1032	104 (9)
		Cropland	831	787	44 (5)
3.	Sub tropical forest	Rice paddy	1177	1054	123 (11)
		Cropland	805	761	44 (4)

CONCLUSION

This paper investigated the land cover changes over the Asian region, which has indicated by comparing current vegetation as imaged by current phenology satellite against a hydro climatic defined potential vegetation that would theoretically exist without human disturbance. By comparing those two yielded maps, we realized that India and China as the center of land cover changes. It also appears in tropics such as Indonesia, Kazakhstan, and Thailand. Some places in Japan, Korea and Mongolia were denoted that the cover changes also occurred but in a relative small area.

Based on E_a calculation, the changes of E_a between current and potential vegetation is around 0 to 12% per year. The 0 value indicates the area where the E_a and land cover has no changed. The lower value (less than 5%) was happened when evergreen broadleaf forest (seasonal) changed to rice paddy. It also occurred when the subtropical rain forest has been changed to cropland. In addition, when the sub tropical rain forest changed to rice paddy, the E_a was decreased by 9%. The highest decreased value (12%) was occurred when the tropical rain forest was changed to rice paddy.

I consider that further research maybe necessary to improved the outcome of this research by using more accurate datasets and research methods in order to obtain better understanding concerning the anthropogenic land cover changes and its influences on hydrological processes.

ACKNOWLEDGEMENT

I deeply appreciate the producers of Time series of Global Monthly Vegetation Cover from NOAA/AVHRR: April 1985-December 1997. NOAA National Climatic Data Center. Published on CD-ROM by NOAA/NESDIS/ NCDC. Additionally, the CRU05 0.5 lat/lon gridded monthly climate data has been supplied by the Climate Impacts Link Project (UK Department of the Environment Contract EPG 1/1/16) on behalf of the Climatic Research Unit, University of East Anglia. We are grateful also for the producers and editors of Global Ecosystem Database version 1.0 CD-ROM. The assistance of Agung Budi Harto, Betty Philip, Ketut Wikantika, and Teguh Prajogo is greatly appreciated.

REFERENCES

Achard F., and Estreguil Ch., 1995, Forest classification of Southeast Asia using NOAA AVHRR data. *Remote Sens. Environ.* 54:198-208.

Ahn, C.H. 1995. *Esti*mate of global land evapotranspiration and water resources using GIS techniques. PhD thesis. Graduate School of Science and Technology. Chiba University.180p.

Ahn, C.H and Tateishi R. 1994. Development of global 30-minute grid potential evapotranspiration dataset. Journal of Japan Society Photogrammetry and Remote Sensing Journal 33(2): 12-21.

Bouwman, A. F., Fung I., Mathew E., and John, J. 1993. Global analysis of the potential for nitrous oxide (N2O) production in natural soils, Global Biogeochemical Cycles, 7: 557-597.

Budyko, M.I., 1974, Climate and life. (translated by D.H.Miller). Academic Press, Inc. New York.

DeFries R., and Townshend, S. J. 1994. NDVI-derived land cover classifications at a global scale. Int. J. Remote Sensing 15 (17): 3567-3586. Special issue on global data sets.

Dorman, J.L., and Sellers, P.J. 1989. A global climatology of albedo, roughness length and stomatal resistance for atmospheric general circulation models as representated by the Simple Biosphere Model (SiB). Journal of Applied Meteorology 28: 833-855.

Jensen, M.E., Burma E.D., Allen, R.G. 1990. Evapotranspiration and irrigation water management, ASCE Manuals and Report on Engineering Practice, 70 p.

Justice, C. O., Townshend, J. R. G., Holben, B. N., and Tucker, C. J. 1985. Analysis of the phenology of global vegetation using meteorological satellite data. Int. J. Remote Sensing 6(8): 1271-1318.

Kira, T. 1945. New climatic zonation in eastern asia as a basis of agricultural geography. Kyoto Imperial University (in Japanese).

Leemans, R. 1990. Global Holdrige life zones. Digital Data. IIASA, Laxenberg, Austria; 10.

Los, S., Justice, C., and Kendall, J. 1994. A Global 10 by 10 NDVI dataset for climate studies, Part I: Derivation of a reduced resolution dataset from the GIMMS global area coverage product of AVHRR. International Journal of Remote Sensing 15: 3493-3518.

Kotoda, K. 1986. Estimation of river basin evapotranspiration. Environmental Research Center Papers, No.8, University of Tsukuba; 66.

Kondoh, A., 1994. Comparison of the evapotranspiration in Monsoon Asia estimated from different methods. J. of Japanese Assoc. Hydrol. Sci., 24: 11-30. (in Japanese with English abstract).

Kondoh, A. 1995. Relationship between the global vegetation index and the evapotranspiration derived from climatological Estimation Methods. J. of the Japan Society of Photogrammetry and Remote Sensing, 34(2): 6-14.

Malingrau, J. P. 1986. Global vegetation dynamics: Satellite observations over Asia. International Journal of Remote Sensing 7(9):1121-1146.

Mathews, E., 1983. Global vegetation and land use: New high-resolution data base for climate studies. Journal of Climatology and Applied Meteorology 22: 474-487.

Olson, J. S. 1994a. Global ecosystem framework-definitations: USGS EROS Data Center Internal Report, Sioux Falls, SD: 37.

Olson, J. S. 1994b. Global ecosystem framework-translation strategy: USGS EROS Data Center Internal report, Sioux Falls, SD: 39p.

Priestley, C. H. B., and R.J. Taylor. 1972. On the assessment of surface heat flux and evaporation using large-scale parameters. Monthly Weather Review 100: 81-92.

Running, S. W., Nemani, R, Hibbard K, and Churkina G. 1996. The influence of land cover change on global terrestrial biogeochemistry. Proceedings of IGBP/BAHC-LUCC Joint Inter-Core Projects Symposium Kyoto, Japan; 6-9.

Tucker, C.J., Townshend, J.R.G., and Goeff, T.E. 1985. African land cover classification using satellite data. Science 277: 369-375.

Tateishi, R., Wen, C. G., and Parera, K. 1997. Global four-minute land cover data set. J. of the Japan Society of Photogrammetry and Remote Sensing 36(4): 62-74.

Townshend, J. R. G., and Justice, C. O. 1986, Analysis of the dynamics of African Vegetation using the Normalized Difference Vegetation Index. Int.J.Remote Sensing 7(11): 1435-1445.

Thornthwaite, C. W. 1948. An approach toward a rational classification of climate. Geogr. Rev. 38: 55-94.

Thornthwaite, C. W., and Mather, J. R. 1957. Instructions and tables for computing potential evapotranspiration and the water balance. Drexel Institute of Technology Laboratory of Climatology. Public*ation in Climatology*, 4(3): 182-203.